A COMPARISON STUDY OF MAGNETIC BEARING CONTROLLERS FOR A FULLY SUSPENDED DYNAMIC SPIN RIG

by

Benjamin Choi, Dexter Johnson, Carlos Morrison and Oral Mehmed

NASA Glenn Research Center, Cleveland, Ohio 44135, U.S.A.

benjamin.choi@grc.nasa.gov, dexter.johnson@grc.nasa.gov
carlos.morrison@grc.nasa.gov, oral.mehmed@grc.nasa.gov

8th International Symposium on Magnetic Bearings

ABSTRACT

NASA Glenn Research Center (GRC) has developed a fully suspended magnetic bearing system for the Dynamic Spin Rig (DSR) that is used to perform vibration tests of turbomachinery blades and components under spinning conditions in a vacuum. Two heteroplolar radial magnetic bearings and a thrust bearing and the associated control system were integrated into the DSR to provide noncontact magnetic suspension and mechanical excitation of the 35 lb vertical rotor with blades to induce turbomachinery blade vibration.

A simple proportional-integral-derivative (PID) controller with a special feature for multidirectional radial excitation worked very well to both support and shake the shaft with blades. However, more advanced controllers were developed and successfully tested to determine the optimal controller in terms of sensor and processing noise reduction, smaller rotor orbits, and energy savings for the system. The test results of a variety of controllers we demonstrated up to the rig's maximum allowable speed of 10,000 rpm are shown.

INTRODUCTION

Today's turbomachinery components have extensive testing requirements and therefore there is a need to provide enhanced testing capabilities (References [2] and [3]). Rotating components are expected to be used at very high rotational speeds, have extended life, and have better static and dynamic properties. The Dynamic Spin Rig (DSR) (see Figure 1) is used to perform research on turbomachinery blades and components under spinning conditions by rotating them in a vacuum chamber (Reference [1]). During rotation the rotor can be vibrated by using two voice-coil type linear electromagnetic shakers that apply axial forces to the rotor. Dynamics measurements are obtained yielding the blade's natural frequencies.

Johnson et al. (References [5] and [6]) replaced the bottom radial ball bearing of the DSR with a radial active magnetic bearing thereby providing magnetic suspension as well as magnetic excitation. This unique system that enables the magnetic bearing to act as a shaker provided an excitation force at critical modes to successfully complete various US engine companies, NASA GRC (Reference [4]), and University of California turbine and/or fan blade damping tests. It was proven that bearing mechanical life was substantially extended and increased flexibility in excitation orientation (direction and phasing) was achieved.

Recently, we upgraded the DSR to have a fully suspended excitation system by replacing the remaining conventional radial ball bearings and the voice-coil type linear electromagnetic shakers. The new magnetic suspension and excitation system can provide longer run times at higher speeds and larger vibration amplitudes for rotating blades. Compared to the existing system, the new system can transmit more vibrational energy into the shaft and thus enable the excitation of higher blade modes observed in turbomachinery. Additionally, the magnetic bearing provides active control of stiffness and damping at the point of action. All of these features enable more useful testing to be performed.

In this paper, for the rotor levitation purpose, a decentralized proportional-integral-derivative (PID) controller and a centralized modal controller were developed first because those were easy to implement, and modern control technique such as Kalman filtering was used to develop a better controller that reduces sensor and processing noise, rotor orbits, and control current noise, which are critical to analyzing experimental damping test results.

TEST FACILITY DESCRIPTION

The DSR provides experimental data for evaluation of vibration analysis methods for rotating systems. Bladed rotors up to 81 cm (32 in.) in diameter can be spun up to 20 000 rpm by a speed regulated air motor. Before installation of the magnetic bearing, electromagnetic shakers were primarily used to apply oscillatory axial forces to the rotor shaft through a thrust bearing. Strain gages, accelerometers, and optical blade-tip vibration sensors provide blade vibration signals.

Figure 2 is a cutaway drawing of the rig with two mechanical bearings supporting the rotor. Shown are the vacuum tank, the air motor drive, two electromagnetic shakers, a multi-blade rotor (with a vertical axis of rotation), a 100-channel slip ring assembly (which is located at the bottom of the rotor and is used to take signals from the rotor). In Figure 3, the magnetic bearing is shown installed in the rig. The vacuum (down to 0.02 psia) reduces the torque required to drive the disk and renders aerodynamic effects negligible.

The radial magnetic bearing is a 4-pole heteropolor type. Each pole has 160 coil turns with an independent PWM amplifier. Its outer diameter is 4.7 in. It is operated using a maximum of 6 A/coil. The backup bearing gap distance is 0.010 in. with a typical operating radial shaft excursion of about 0.005 in.

An analysis shows that the rig is able to run up to 20 000 rpm without exceeding the stress limit of the bearing laminations. Up to date of this publication, running at more than 10,000 rpm is not recommended until a complete health monitoring system for the rig is installed. Therefore, all of the experimental data in this paper have been shown up to 10,000 rpm.

CONTROL SYSTEM

The control system uses both classical and modern control techniques, which are implemented with the MS-DOS Turbo ANSI C programming language on a Pentium I/200MHz PC. Datel A/D input board and Metrabyte D/A output board were used to get sensor signals and to send out the control command signals to power amplifiers.

Figure 4 shows the control system block diagram that includes all of the excitation and suspension elements which represent the system. The controller has two primary components. One component provides the magnetic bearing suspension and the other provides the excitation (see References [5] and [6] for the details). This paper focused on looking for an optimal controller for the magnetic suspension that can remove unnecessary high frequency signals for the damping test analysis.

A user-friendly controller cockpit window allows modification of the magnetic bearing parameters such as bias, stiffness, damping, and integral gain for PID controller. It has a switch for a decentralized PID controller,

centralized modal controller, control force integral feedback, and Kalman estimator. A safe gain feature is triggered to protect the bearing system at higher speeds when the rotor orbit exceeds the predefined orbit size. Also, a whirling feature was implemented to investigate the dynamic behavior of the magnetically suspended rotor system as well as to check the backup bearings before the actual rotation. Whirling orbit size, starting angle, and the center point of the orbit are all user defined and aid in investigating the bounce mode and tilting mode. All of the above-mentioned features can be controlled separately for lower and upper bearings. In addition to an external comprehensive data collecting system, a simple data acquisition capability was added to the control cockpit window to monitor the system performance.

Decentralized PD and PID Controller

The first controller we tested was a simple PD controller because it was easy to implement as

$$i(x) = -\frac{(k + k_x)x + d\dot{x}}{k_i} \qquad (1)$$

where a proportional gain feedback $P = (k + k_x)/k_i$ and a differentiating feedback $D = d/k_i$. The proportional gain includes a term to offset the negative bearing stiffness k_x and one to produce the actual bearing net stiffness k. The differentiating component controls the damping of oscillations. This control current force was added to the bias current to obtain a linear relation between force and control current. At critical modes, even a simple decentralized PD controller was sufficient to suppress the vibration amplitude.

Next we tested an integral feedback (Reference [7]) scheme, which was easily implemented with the PD controller. In practice it is often desirable to keep a given rotor position independent of changes in the load. An additional integrating feedback-path in the controller compensated well for such change. Any deviation of the position x is integrated over time slowly and added to the feedback until the error signal e becomes zero.

In order to determine what combination of gains are useful and produce stable operation, a stability map was obtained experimentally by observing and recording what gain combinations produced instability. These gains show a stability surface under which stable operation of the system is achieved. The gain set in the middle range was selected and plugged into the controller as a safe gain set, which is triggered to protect the bearing system at higher speeds when the rotor orbit exceeds the predefined orbit size.

A frequency domain representation of the system's dynamic characteristic gives another perspective of the system. A transfer function between the excitation sig-

nal and the shaft position signal gives a spectral profile that indicates how well we can transmit energy to the system.

Figure 9 shows the rotor orbit and control current for each coil in operation at 0 rpm up to 10,000 rpm. The rotor orbits over the operating rage were small and solid, but significant high frequency noise level remained at the rotor orbit and control current. Figures 6 and 7 show the auto power spectrum of the rotor orbit and control current, respectively. As shown in Figure 7, the PD control current contains significant amount of high frequency noise.

Centralized Modal Controller

In order to have more vibration amplitude suppression and stable rotor orbits at critical modes, we tested a centralized modal controller that consists of two parts:

Rigid Body Translation. The decentralized forces are

$$
\begin{aligned}
F_1 &= -k_1 x_1 - c_1 \dot{x}_1 \\
F_2 &= -k_2 x_2 - c_2 \dot{x}_2
\end{aligned}
\tag{2}
$$

where F_1 and F_2 are the x-axis forces from the top and bottom radial bearings, respectively. The average horizontal translation of the rotor along the center of mass is $x_{av} = (x_1 + x_2)/2$. Hence, the force on each side to compensate the horizontal deviation from the set point is

$$
F_{tr1,2} = -\frac{1}{2}\left((k_1 + k_2) x_{av} - (c_1 + c_2) \dot{x}_{av} \right)
\tag{3}
$$

Rigid Body Rotation. The tilt angle of the rotor with respect to the vertical y-axis is $\theta = (x_2 - x_1)/l$ where l is the distance between the centers of the top and bottom radial bearings. The control torque to be created at the tilt angle θ is

$$
T = -k_{tilt}\theta - c_{tilt}\dot{\theta}
\tag{4}
$$

where the rotational stiffness $k_{tilt} = (k_1 + k_2) \cdot l^2 / 4$ and the rotational damping $c_{tilt} = (c_1 + c_2) \cdot l^2 / 4$. The control forces to be exerted are $F_{rot1,2} = T/l$. Thus, combining $F_{rot1,2}$ with Equation (3) gives the centralized control force from each radial bearing:

$$
F_{mod1,2} = -\frac{1}{4}\left(\begin{aligned} &(k_1 + k_2)(x_1 + x_2) + (k_1 + k_2) \cdot l \cdot \theta \\ &+ (c_1 + c_2) \cdot l \cdot \dot{\theta} \end{aligned} \right)
\tag{5}
$$

The centralized y-axis forces can be obtained in the exact same way. When we tested this controller

throughout the operating range, the rotor orbit and control current level over the operating range were almost the same as the PD controller except at the first rigid body mode (about 2,700 rpm). Since the PD controller worked well even at the first mode, for this specific application, we couldn't see a big advantage.

Control Force Integral Feedback

Next we tested a control force integral feedback, which is somewhat similar to the integral action of the PID control law described earlier. Simply adding an integral of the control force output to the output moves the shaft to the magnetic force center so that an average control output can be minimized. Brown (Reference [8]) successfully demonstrated this concept on a magnetic-bearing-supported energy storage flywheel at NASA GRC. It was proven that this technique maintained near zero average control current throughout the speed range without any operator attention.

When the control force integral feedback was activated, the magnetic force center, geometric backup bearing center, and zero sensor position were almost matched. In other words, the new DSR has almost perfect concentricity and alignment of the bearing system.

When the control force integral was activated, the control force was integrated over time slowly and added to the feedback force output until the time-averaged control force becomes zero. The test results showed almost the same orbit and control current as those in the PID controller.

LQG (Linear-Quadratic-Gaussian) Regulator

All of the above-mentioned controllers worked well in terms of the rotor orbit (position control) and control current level throughout the operating range up to 10,000 rpm. However, they could not meet the low noise requirement of the new DSR that should deliver clean blade-vibration signals. Hence we wish to reduce high frequency magnetic bearing control noise, which may couple into the blade vibration measuring circuits, which is critical to good experimental damping test results.

To resolve this problem, a simple LQG regulator was developed based on a simple 2nd order experimental plant model that approximates the rotor and magnetic bearing system. It was successfully demonstrated up to 10,000 rpm, significantly reducing the noise level and maintaining predefined gains throughout the speed range. This control law doesn't use differentiation of the measured displacement signal, but a state estimation through a Kalman filter. Also it is quite useful in practice to trade off regulation performance with control effort for a given design specification. A simple design procedure is described as follows.

With the rotor levitated, a transfer function between

the control force command signal and the shaft position signal was measured as shown in Figure 5. A simple 2nd order open-loop plant model was approximated by neglecting higher order dynamics beyond the first natural frequency as

$$tf(x/u) = \frac{k}{(as^2 - 1)} \quad (6)$$

where $k = 1.19$ and the time constant $a = 1/w_n$. Based on this plant model with $w_n = 45 Hz$, a full state feed back matrix F was computed first given our design specification, and the LQG-design was then followed in such a way as to minimize a cost function J defined as the integral over weighted squares of state variables and control variables according to

$$J(u) = \int_0^\infty \left(x^T Q x + u^T R u + 2x^T N u\right) dt \quad (7)$$

In our design specification, the respective weighting ratio for the square matrices Q and R is 1 to 10. We assumed no coupled effect between x and u, thereby the third term was neglected. We combined this with the optimal gain matrix F to have a simple LQG regulator and then converted it into the discrete-time model using a sample time $T_s = 80 \mu s$.

Compared to the PD controller shown in Figures 6 and 7, the LQG controller reduced rotor orbit by about 50% after 35 Hz, however it significantly reduced the high frequency control noise level. Also, much clean rotor orbits over the operating range were achieved shown in Figure 9. Figure 8 shows the controller transfer functions of PD and LQG regulator. It seems that the LQG regulator has the same P (stiffness) and D (damping) values as in the PD controller, but with a roll-off at about 150 Hz. A simple PD controller with a low-pass filter, which has the exact same transfer function as the LQG regulator will be tested later to verify this observation.

SUMMARY
A fully suspended Dynamic Spin Rig (DSR) was developed to provide blade vibration excitation, and shaft suspension and control. The rig was upgraded by replacing conventional ball bearings and mechanical shakers with the 5-axis magnetic bearing system (two radial and one thrust bearings), thereby providing longer run times at higher speeds and larger vibration amplitudes for rotating blade tests. Various control techniques were investigated up to the maximum allowable speed of 10,000 rpm to determine the optimal controller for the DSR. All the tested controllers worked well in terms of rotor orbit and control current level throughout the speed range. However, the LQG regulator showed the best performance in terms of noise reduction, control energy savings, and rotor orbit in relatively higher frequency region. In the near future, a PID controller with a low pass filter and an H∞ synthesis controller will be tested to further reduce noise level and to improve the system robustness.

REFERENCES
1. Brown, G.V., Kielb, R.E., Meyn, E.H., Morris, R.E., Posta, S.J., "Lewis Research Center Spin Rig and Its Use in Vibration Analysis of Rotating Systems." NASA TP–2304, May 1984.
2. Kosmatka, J.B., Lapid, A.J., and Mehmed, O., "Behavior of Spinning Laminated Composite Plates with Initial Twist-Experimental Investigation." Proceedings of the ASME Winter Meeting, November 1992.
3. Kosmatka, J.B., Lapid, A.J., "The Experimental Behavior of Spinning Pretwisted Laminated Composite Plates." Department of Applied Mechanics and Engineering Services, University of California, San Diego. Final Report on a Research Project Funded through NASA Research Grant Number NCC 3-173. Report No. SSRP-93/10.
4. Mehmed, O., Kosmatka, J.B., "Damping Experiment of Spinning Composite Plates With Embedded Viscoelastic Material," Physics and Process Modeling (PPM) and Other Propulsion R&T, Cleveland, Ohio, May 1, 1997, NASA CP–10193, Volume II.
5. Johnson, D., Mehmed, O., Brown, G.V., "Magnetic Excitation for Spin Vibration Testing," Physics and Process Modeling (PPM) and Other Propulsion R&T, Cleveland, Ohio, May 1, 1997, NASA CP–10193, Volume II.
6. Johnson, D., Brown, G.V., Mehmed, O., "Magnetic Suspension and Excitation System for Spin Vibration Testing of Turbomachinery Blades," AIAA-98-1851.
7. Schweitzer, G., Bleuler, H., Traxler, A., *Active Magnetic Bearings*, vdf Hochschulverlag AG an der ETH Zurich, 1994.
8. Brown, G.V., "DC Control Effort Minimized for Magnetic Bearing Supported Shaft," NASA/TM-2001-210605, 2001.
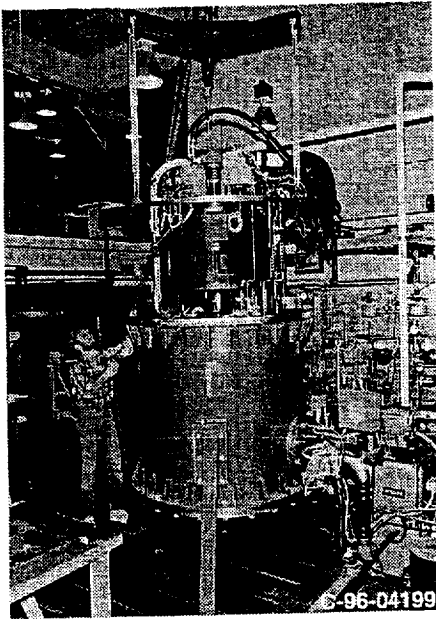
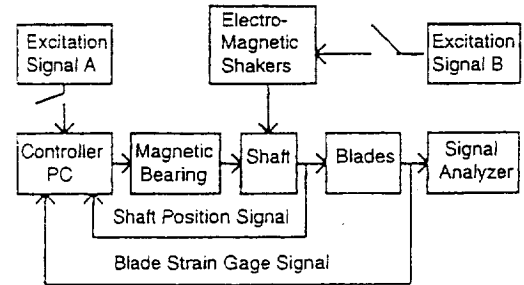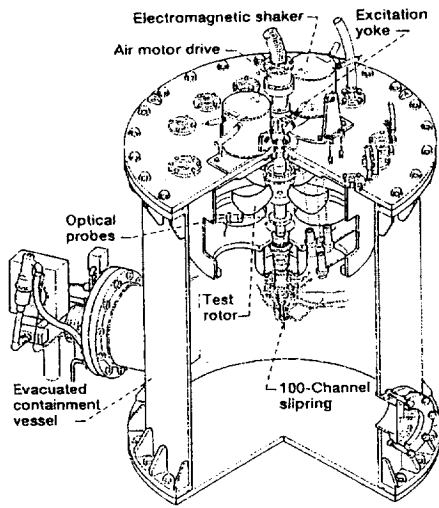FIGURE 1: Dynamic Spin Rig Facility.

FIGURE 2: Cutaway drawing of Dynamic Spin Rig.
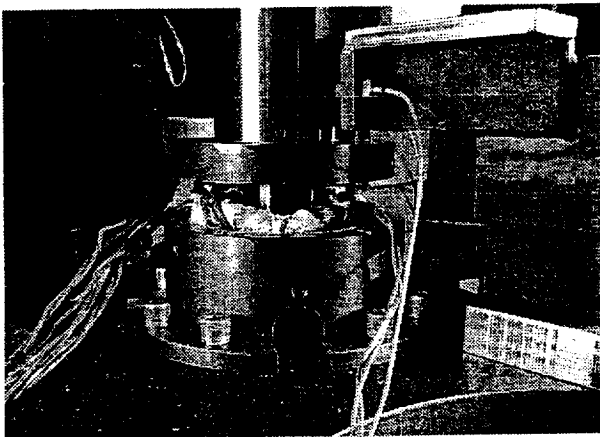
FIGURE 3: Lower magnetic bearing installed in Dynamic Spin Rig.
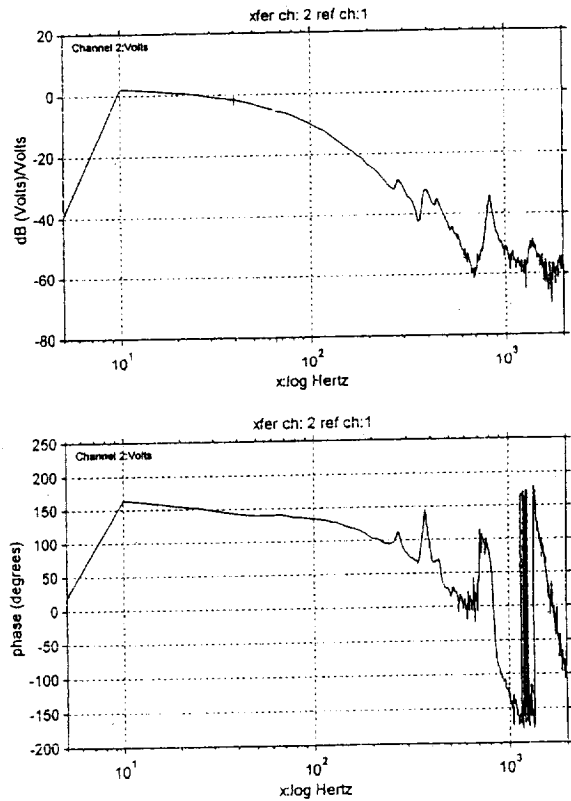

FIGURE 4: Block diagram for Dynamic Spin Rig excitation system.

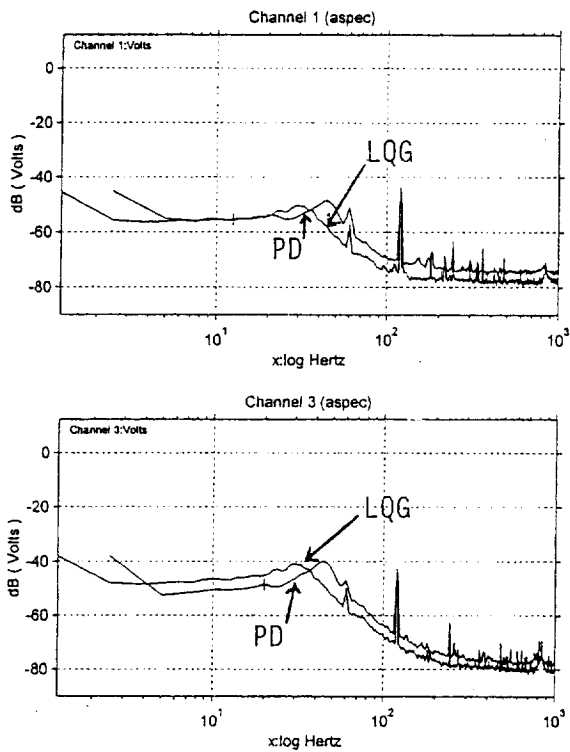FIGURE 5: Experimental transfer function of open-loop plant model at the upper radial magnetic bearing.

Channel 1 (aspec)

LQG

PD

Channel 3 (aspec)

LQG

PD

FIGURE 6: Power spectrum of the upper- and lower-rotor orbits with the PD controller and LQG regulator, respectively.

xfer ch: 2 ref ch:1
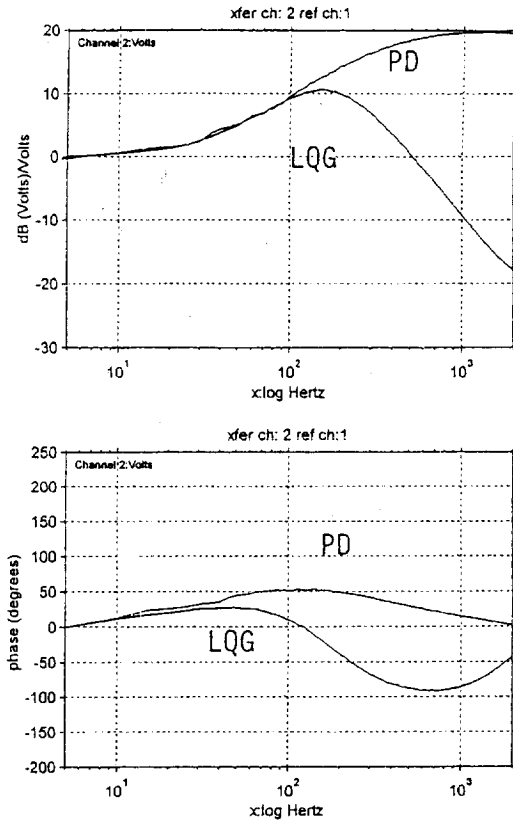
PD

LQG

xfer ch: 2 ref ch:1

PD

LQG

FIGURE 8: Bode plot of the PD controller and LQG regulator for the top radial bearing.
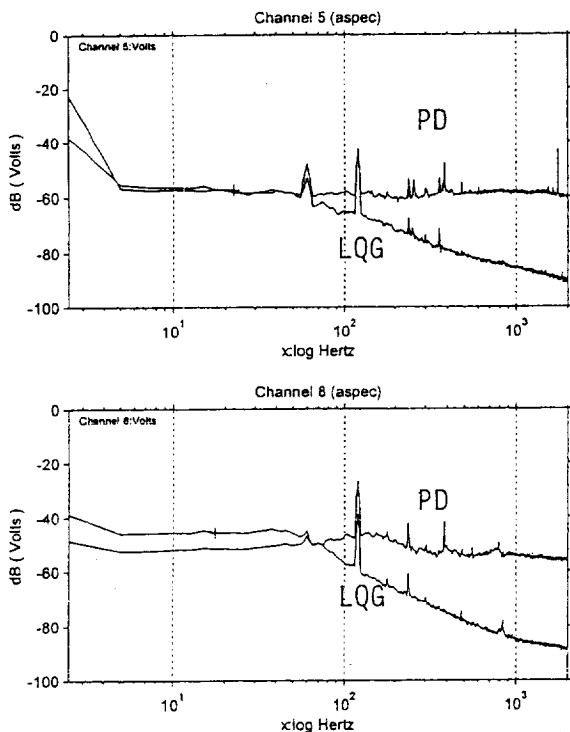
Channel 5 (aspec)

PD

LQG

Channel 6 (aspec)

PD

LQG

FIGURE 7: Power spectrum of the upper- and lower-control currents with the PD controller and LQG regulator, respectively.

(PD)   (LQG)

1k

2.6k
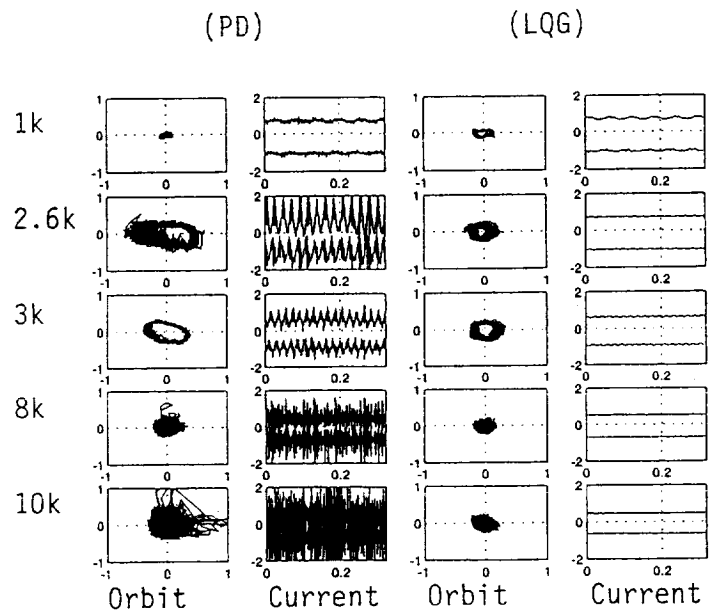
3k

8k

10k

Orbit   Current   Orbit   Current

FIGURE 9: Rotor orbit and control current of the top radial bearing throughout the operating range.